

Structural Change of Myosin Motor Domain and Nucleotide Dissociation: Molecular Dynamics Simulation by “Dual-Gō Model”

Fumiko Takagi*

*Formation of Soft Nanomachines, Core Research for Evolutional Science and Technology,
Japan Science and Technology Agency, Suita, Osaka, Japan and
Cybermedia Center Osaka University, Toyonaka, Osaka, Japan*

Macoto Kikuchi†

*Cybermedia Center Osaka University, Toyonaka, Osaka, Japan and
Formation of Soft Nanomachines, Core Research for Evolutional Science and Technology,
Japan Science and Technology Agency, Suita, Osaka, Japan*

(Dated: February 9, 2020)

We investigate the structural relaxation of myosin motor domain from the pre-powerstroke state to the near-rigor state by molecular dynamics simulation. In order to describe the structural change, we propose “dual Go-model”, a variant of Go-like model. Nucleotide dissociation process is also observed with a coarse-grained nucleotide as well as a coarse-grained protein included in the simulation. We found that the myosin structural relaxation toward near-rigor conformation could not complete before the nucleotide dissociation. Moreover the relaxation and the dissociation occur cooperatively when the nucleotide was tightly bound to myosin head.

Introduction

Mechanism of biomolecular motors has been one of the largest topics of biophysics. Among a number of such systems that have been found so far, the actomyosin motor is of a particular interest, because it is responsible to muscle contraction and cellular movements in eukaryotic cells. Myosin moves unidirectionally along the actin filament using chemical energy released by ATP hydrolysis [1, 2, 3]. It is widely recognized that efficiency of this energy conversion is very high compared to macroscopic artificial machines, in spite of the fact that biomolecular motors work under noisy environment in cells. In fact, the free-energy released at each ATP hydrolysis is only about $20k_B T$ so that the thermal fluctuations should be appreciable. Although recent progress in experimental techniques of imaging and of nano-manipulation has been making single molecule observation possible, the moving mechanism of actomyosin motor is still open.

There has been a long standing controversy between tight-coupling (lever-arm) model and loose-coupling model. X-ray crystallographic studies revealed that the angle of the neck domain relative to the motor domain changes depending on the nucleotide state. The “lever-arm model” was proposed based on these observations, in which the structural change of myosin is tightly coupled with the ATP hydrolysis cycle and directly causes the stepwise sliding motion. It was shown, however, that the sliding distance of a myosin along the actin filament per ATP at the muscle contraction can be much longer than the displacement predicted by the ‘lever-arm’-like structural change of a single myosin[4]. Moreover, it is

questionable if a material as soft as proteins can switch its conformation accurately like a macroscopic machine under thermal fluctuations.

In the “loose coupling” picture, in contrast, the structural change does not always correspond to a step in a one to one manner; the motion is intrinsically stochastic and thermal fluctuation is an essential ingredient for its mechanism[5]. The simplest class of models that realizes the loose coupling mechanism are based on thermal ratchet, in which a myosin is treated as a Brownian particle that moves along a periodic and asymmetric potential under both thermal noise and non-thermal perturbation [6, 7]. Although ratchet systems can, in fact, exhibit unidirectional flow in the noisy environment, a high efficiency comparable to that of the acto-myosin system is found difficult to achieve using only a simple ratchet system. Even if the ratchet models are supposed to express some essence of the mechanism of biomolecular motor, they are too much simplified and we should say that a connection to the real acto-myosin system is rather vague. In particular, since the myosin is expressed as a particle, effect of its conformational change is taken into account, at best, only implicitly. A somewhat more realistic modelling is desirable that can reflect the chain conformation.

Recently, it was revealed by single molecule experiments that the chemo-mechanical cycle of the myosin head is controlled by a load on the acto-myosin crossbridge[8, 9, 10]. The observation suggested that ADP release rate from the myosin head depends on the force acting on myosin; namely, the chemical reaction rate varies with the deformation of the myosin. If the myosin head indeed acts as such a “strain sensor”, what would be recalled is a classical model by A. Huxley [11]; in this model the myosin head is supposed to undergo Brownian motion and to change into a tightly bound state to the actin filament triggered by a structure de-

*Electronic address: fumiko@cp.cmc.osaka-u.ac.jp

†Electronic address: kikuchi@cmc.osaka-u.ac.jp

pendent chemical reaction.

Relationship between structure and function of proteins has long been paid attention to. So far its static aspects have been mainly considered, for example, classical “lock and key” model of enzyme. Recently, the role of structural fluctuation, or more drastic structural change including “partial unfolding”, on protein functions has been becoming a subject of growing interest. Although there have been many experimental studies to clarify the dynamical process of protein function, it is still difficult to observe the structural change with high resolution both in space and time. Computer simulations serve as possible alternatives. Typical computational studies treated equilibrium fluctuation near crystal structure using all-atom model [12, 13] or elastic network model [14]; although these type of simulations cannot deal with large-scale structural change, it was found in some cases that the low-frequency fluctuation modes are consistent with the direction of motion of structural change that is considered as function-associated.

Some attempts have been made to simulate larger structural change beyond the elastic regime using a class of models called Gō-like model [15]. According to the recently developed theory of (spontaneous) protein folding, the protein energy landscape has a funnel-like global shape toward the native structure. Gō-like model is certainly the simplest class of models that can realize this funnel-like landscape[16, 17] and has successfully described small globular proteins or, furthermore, more complex proteins. It, however, is not suitable to study conformational change of myosin head between two conformations, because only the interaction between the pairs of residues that contact in the native state are taken into account; conformation other than the native state is made too unstable as a result. Thus a model is desirable that two conformations can be embedded. Here we introduce a new model bearing this property as a variant of Gō-like model.

In this article, we investigate dynamics of the myosin conformational change from the pre-powerstroke state to the near-rigor state by molecular dynamics simulation. This process is called “powerstroke” because the angle of lever-arm changes remarkably, and it is considered that this structural change directly causes the force generation in lever-arm model. In order to describe the structural change, we propose ”dual Gō-model”. Dissociation process of the nucleotide that accompanies the conformational change is also involved in the simulation by introducing a coarse-grained nucleotide as well as a coarse-grained protein. To our knowledge, the ligand at the binding site has not been explicitly considered in coarse-grained protein simulations, because the primary role of ATP is considered to release chemical energy through hydrolysis. We, however, consider that presence or absence of nucleotide in the binding site would affects the structural fluctuation profoundly. So it is important to perform simulation including nucleotide.

(a) structure-1: near-rigor (b) structure-2: pre-powerstroke

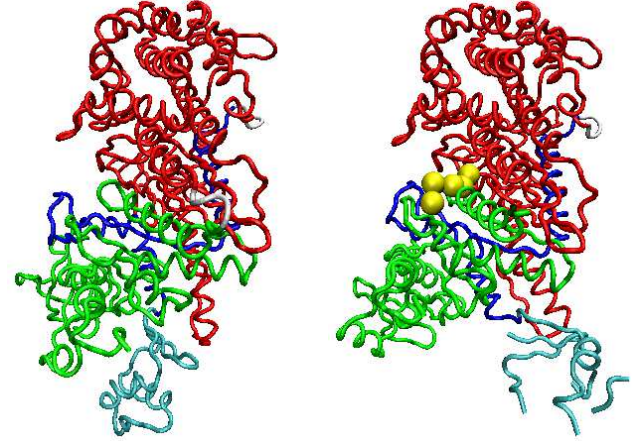


FIG. 1: We choose (a) near-rigor structure, 1Q5G, and (b) pre-powerstroke structure, 1VOM for structure-1 and 2, respectively. 1VOM contains the ADP- P_i analogs ADP- VO_4 (yellow). There are the N-terminal (green), 50 kDa subdomain (red) and the converter (cyan) included in C-terminal subdomain (blue) that is connected to the lever arm.

Results

First, we introduce “dual Gō-model”. While only the native structure is taken as a reference structure for the potential energy function in standard Gō-like models, we modify it to take two reference structures, structure-1 and structure-2, in the effective potential. For the interaction between “native-contact-pair”, each potential energy function has two minima corresponding to two reference structures. For studying the relaxation process from structure-2 to structure-1, the minimum corresponding to structure-2 is given a slightly higher energy than that of structure-1 in order to make structure-1 more stable. In the present study, we use a model based on one of the C_α Gō-like models [18, 19], which involves local interactions such as bond length, bond angle and dihedral angle interaction as well as the native-contact interaction. For these local interactions, we set that each potential energy function has two minima of the same depth corresponding to two reference structures.

As reference structures, we choose x-ray crystal structures of *Dictyostelium discoideum* myosin II: the near-rigor structure without nucleotide, 1Q5G[20] for structure-1 and the pre-powerstroke structure with ADP- P_i analog, 1VOM[21] for structure-2 (Fig.1). Initial structure is the pre-powerstroke structure with a coarse-grained nucleotide (Fig.2) located at the nucleotide binding site.

Typical time courses of dRMSD are shown in Fig. 3. dRMSD from near-rigor structure is defined as

$$dRMSD = \sqrt{\frac{2}{N(N-1)} \sum_{i < j} (r_{ij} - r_{ij}^{(1)})^2}, \quad (1)$$

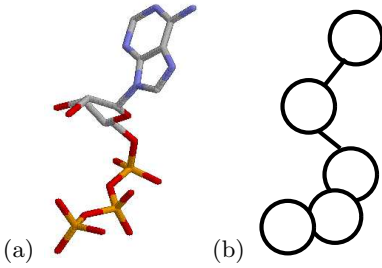
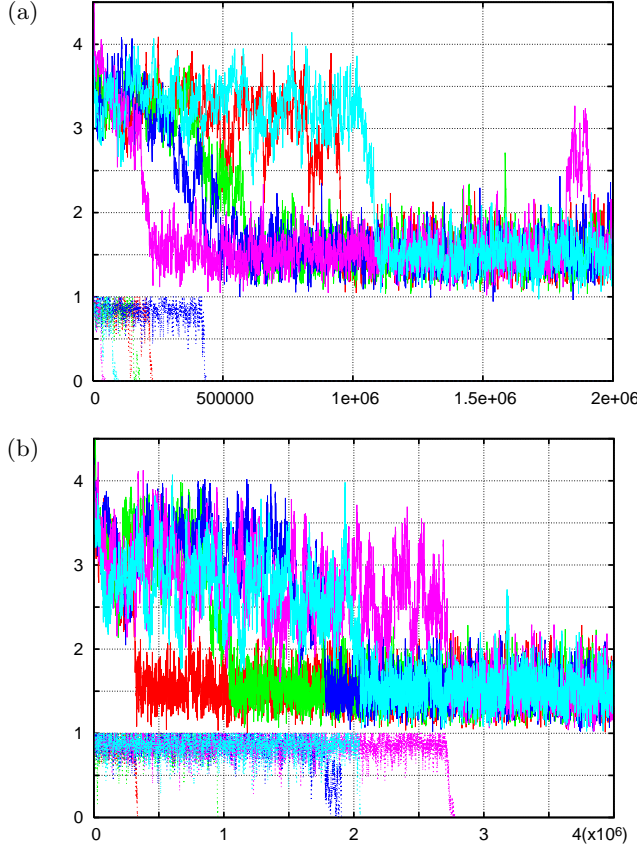
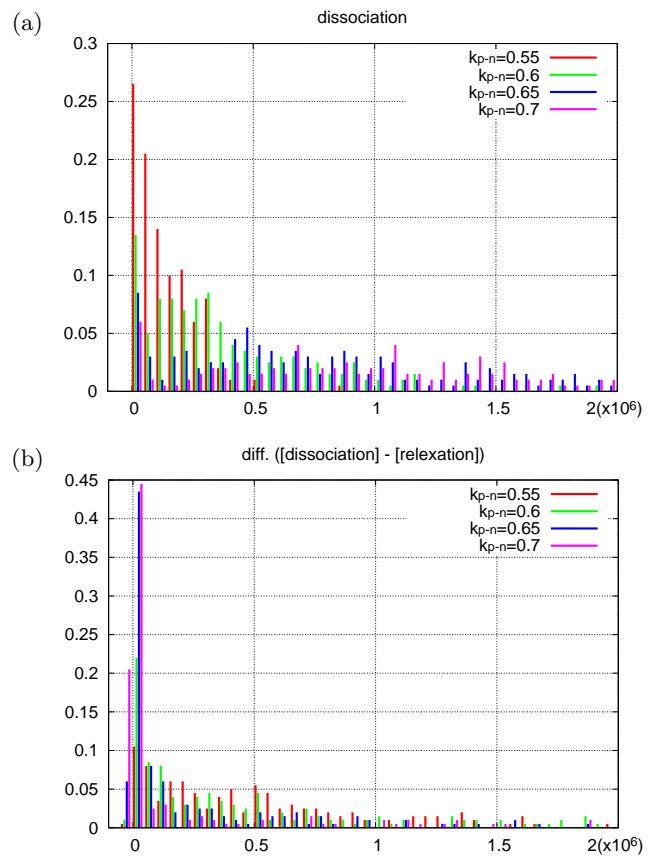


FIG. 2: (a) ATP and (b) coarse-grained ATP.

FIG. 3: Relaxation time courses of dRMSD (from 1Q5G) (solid line) and Q_{nucl} (dotted line) for five trajectories are shown. Different runs are distinguished by colors. (a) $k_{\text{p-n}} = 0.6$, (b) $k_{\text{p-n}} = 0.7$

in which $r_{ij} = \mathbf{r}_{ij} = \mathbf{r} - \mathbf{r}_j$ is the distance between C_α carbons of i and j residues in the given conformation, and $r_{ij}^{(1)}$ indicates their distance in the structure-1, near-rigor structure. At initial conformation, $\text{dRMSD} \sim 3.9 \text{ \AA}$, and decreases rapidly to $\sim 3 \text{ \AA}$, and stays there for a while. We thus observe an “intermediate state” in the relaxation process. The conformation eventually relaxes into the final state, $\text{dRMSD} \sim 1.5 \text{ \AA}$. The myosin conformation is considered to be near-rigor state when $\text{dRMSD} \sim 1.5 \text{ \AA}$.

In order to characterize the state of the nucleotide

FIG. 4: Histogram of the number of steps before dissociation (a) and delay of the relaxation after the dissociation (b) from 200 independent runs for each $k_{\text{p-n}}$.

binding, we introduce an index $Q_{\text{nucl}}(\Gamma)$; we count how many of the “nucleotide-contact” that is formed in structure-2 (pre-powerstroke) remains in a given conformation Γ . Then $Q_{\text{nucl}}(\Gamma)$ is defined as this number divided by a number of the nucleotide-contact in structure-2. $Q_{\text{nucl}} = 1$ when a nucleotide is bound, and $Q_{\text{nucl}} = 0$ if nucleotide binding site is empty. Time courses of Q_{nucl} are shown in Fig.3 for $k_{\text{p-n}} = 0.6$ (a) and 0.7 (b), where $k_{\text{p-n}}$ is a strength parameter of protein-nucleotide interaction. Fig.3 shows that the structural relaxation occurs after or, at earliest, in coincidence with the nucleotide dissociation. Furthermore, the relaxation tends to synchronize with the dissociation as $k_{\text{p-n}}$ increases. To clarify $k_{\text{p-n}}$ dependency of the synchronization, we made the histograms of τ_d and of $\Delta\tau = \tau_d - \tau_r$ from 200 independent runs for each value of $k_{\text{p-n}}$, where τ_d is number of steps taken before the nucleotide dissociates, τ_r is number of steps taken before the conformation relaxes to the near-rigor state, and $\Delta\tau$ means a delay of the relaxation after the dissociation takes place(Fig. 4). For small $k_{\text{p-n}}$, both the histograms of τ_d and that of $\Delta\tau$ show exponential decay, that is, the nucleotide dissociation and the relaxation of the myosin conformation are considered to be decoupled. For larger $k_{\text{p-n}}$, on the other hand, the

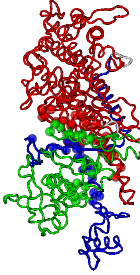


FIG. 5: Residues included in the contacts that are formed at the final relaxation to near-rigor.

histograms of τ_d can not be fitted to an exponential decay. Also, averages of τ_d are shifted to the right and the delays $\Delta\tau$ become shorter; namely, the nucleotide is unbound later and the conformational relaxation tends to occur immediately after the nucleotide dissociation. For $k_{p-n} = 0.7$, dissociation and relaxation occurs nearly simultaneously in over 60% of 200 trajectories. Note that apparent “ $\Delta\tau < 0$ cases” are just due to a numerical ambiguity of τ_d and τ_r and they actually correspond to coincidental dissociation-relaxation.

As shown in Fig.3, the myosin motor domain in the pre-powerstroke conformation relaxes at first into the intermediate state and then to the near-rigor conformation. The largest difference of the intermediate state from the initial (pre-powerstroke) conformation is in a relative position of the converter domain to the other subdomains; the relative positions among other subdomains (for example, N-term. & 50kDa) are basically kept similar to those in the pre-powerstroke conformation. The average dRMSD of the intermediate state varies slightly with the parameter k_{p-n} , reflecting a little difference of the relative position of the converter to the other subdomain.

Some of the native contacts of structure-1 are not formed until the conformation finally relaxes to the near-rigor state. Fig.5 shows residues included in these contacts. They are concentrated at the boundary between N-terminal and 50kDa subdomain, that is, the region around the nucleotide binding site. Thus what goes on in the final relaxation process is rearrangement of the N-terminal subdomain against the other part.

As mentioned above, the myosin motor domain relaxes to the near-rigor conformation only after the dissociation of nucleotide and not before. Thus it seems that the nucleotide is required to be unbound for the final relaxation to occur. This observation leads to a speculation that the nucleotide blocks the deformation of myosin around the nucleotide binding site by its volume. To confirm this, we attempted “the nucleotide-free and constrained simulation”. In this simulation, in stead of explicit inclusion of the nucleotide molecule, the relative positions of

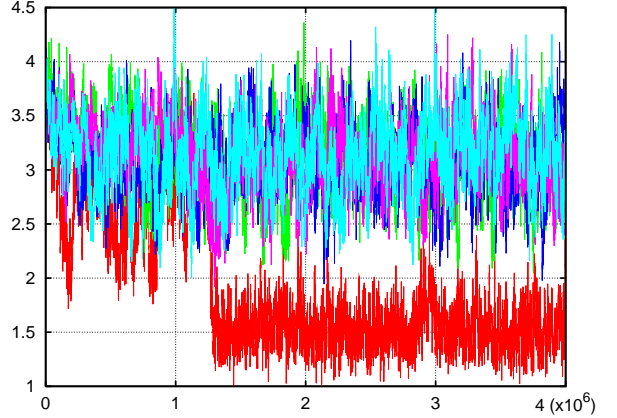


FIG. 6: Time sequence of dRMSD. Red line is trajectory of no-constraint simulation, and the others are trajectories of simulations in which nucleotide binding site are constrained.

the residues that would contact with nucleotide are constrained by virtual bonds to keep the pre-powerstroke form. Fig.6 shows time courses obtained by the simulations. We find that the conformation stays at the intermediate state and the relaxation toward the near-rigor state is not completed.

Discussions

The relaxation simulation using the coarse-grained myosin and nucleotide have shown that the relaxation of the myosin motor domain to the near-rigor conformation does not occur before the nucleotide dissociation. Ishijima *et al.*[22] showed by simultaneous observation of ADP releases and mechanical events that the force is generated in coincidence with or several hundreds of milliseconds after the ADP dissociation. The present results are consistent with their experimental findings if the force generation is preceded by the structural relaxation. Moreover, the results from the constrained simulations in which the nucleotide binding effect are included effectively as the constraints on conformations also indicate that the relaxation is indeed prevented if the nucleotide can not dissociate. Based on these observations, now we suggest a possibility that the primary role of the nucleotide in the myosin “powerstroke” process is just to suppress the relaxation through blocking the deformation around the nucleotide binding site by its volume, and that the hydrolysis is required to alter the affinity of the nucleotide to the binding site rather than to release the chemical energy. In particular, the present simulations have shown that the structural relaxation synchronizes with the nucleotide dissociation when the nucleotide is tightly bound to the myosin head. In other words, the nucleotide dissociation occurs cooperatively with the subdomain motion in the myosin motor domain. This strong coupling of deformation and dis-

sociation seems to be relevant to the function of “strain sensor” in which the nucleotide dissociation(/association) is controlled by the strain induced by an external force. Furthermore, the correlation changes depending on the binding strength, k_{p-n} ; the relaxation is coupled with the dissociation tightly for strong binding condition and only loosely for weak binding condition. Experimental studies have revealed a large kinetic diversity among myosins [23, 24]. Present results on the dependence of the correlation on the binding affinity of nucleotide to myosin may explain such difference in kinetics.

The intermediate state observed in the relaxation process should also be given som discussion. Although several intermediate states are known to exist from kinetic experiments their structural aspects are little known except for ADP·Pi state. Shin et al.[25] reported that there are two “pre-powerstroke” conformations, based on their FRET study; while one corresponds to the crystal structure of the complex with ADP·Pi analog, another has not yet been seen by crystallography. We found that the average structure of the intermediate observed in the present study is consistent with the latter conformation.

The constrained simulation using virtual bonds instead of the coarse-grained nucleotide could revealed a role of the nucleotide on the myosin structural change. Similar approach will also be effective in understanding the actin activation of ATPase or other effects of ligands.

Model and Methods

“Dual Gō-model” is a variant of a C_α Gō-like model[18, 19]. A protein chain is consisted of spherical beads that represents C_α atoms of amino acid residues connected via virtual bonds. In conventional Gō-like models, only amino acid pairs that contact in the native conformation are assigned effective energy. Only some pairs are assigned effective energy also in the dual Gō-model, but now the effective energy function takes two reference structures, structure-1 and structure-2, to describe conformational change from structure-2 to structure-1. Nucleotide molecule is also expressed as connected beads.

Total energy of the system U_{total} consists of 3 terms,

$$U_{\text{total}} = U_p + U_n + U_{p-n}, \quad (2)$$

where U_p is the intra-protein interaction, U_n is the intra-nucleotide interaction, and U_{p-n} is the interaction between protein and nucleotide.

The effective energy of protein, U_p , at a conformation Γ is given as

$$U_p(\Gamma, \Gamma^{(1)}, \Gamma^{(2)}) = U^b + U^\theta + U^\phi + U^{\text{nc}} + U^{\text{nnc}}. \quad (3)$$

where $\Gamma^{(1)}$ and $\Gamma^{(2)}$ stand for conformations of two reference structures. Each term of eq.3 is the following:

$$U^z = \sum_i \min\{V_z^{(1)}(z_i), V_z^{(2)}(z_i)\}, \quad (4)$$

$$U^{\text{nc}} = \sum_{j < i-3}^{\text{native contact}} \min\{V_{\text{nc}}^{(1)}(\mathbf{r}_{ij}), C_{12}V_{\text{nc}}^{(2)}(\mathbf{r}_{ij})\}, \quad (5)$$

$$U^{\text{nnc}} = \sum_{j < i-3}^{\text{non-native contact}} V_{ij}^{\text{nnc}}(\mathbf{r}_{ij}). \quad (6)$$

where (1) and (2) again indicate the reference conformations. In these equations, z stands for b , θ or ϕ . b_i is the virtual bond length between two adjacent C_α carbons, $b_i = |\mathbf{b}_i| = |\mathbf{r}_{i+1} - \mathbf{r}_i|$, where \mathbf{r}_i is the position of the i -th amino acid. θ_i is the angle between two adjacent virtual bonds, \mathbf{b}_{i-1} and \mathbf{b}_i , and $\cos \theta_i = \mathbf{b}_{i-1} \cdot \mathbf{b}_i / b_{i-1} b_i$. ϕ_i is the i -th dihedral angle around \mathbf{b}_i . $\mathbf{r}_{ij} = \mathbf{r}_i - \mathbf{r}_j$. The first three terms of eq.3 provide local interactions. The last two terms are interactions between nonlocal pairs that are distant along the chain.

$$V_b^{(\alpha)}(b_i) = k_b(b_i - b_i^{(\alpha)})^2 \quad (7)$$

$$V_\theta^{(\alpha)}(\theta_i) = k_\theta(\theta_i - \theta_i^{(\alpha)})^2 \quad (8)$$

$$V_\phi^{(\alpha)}(\phi_i) = k_\phi \left[\left(1 - \cos(\phi_i - \phi_i^{(\alpha)})\right) + \frac{1}{2} \left(1 - \cos 3(\phi_i - \phi_i^{(\alpha)})\right) \right] \quad (9)$$

$$V_{\text{nc}}^{(\alpha)}(\mathbf{r}_{ij}) = k_{\text{nc}} \left[5 \left(\frac{r_{ij}^{(\alpha)}}{\mathbf{r}_{ij}} \right)^{12} - 6 \left(\frac{r_{ij}^{(\alpha)}}{\mathbf{r}_{ij}} \right)^{10} \right] \quad (10)$$

$$V_{ij}^{\text{nnc}}(\mathbf{r}_{ij}) = k_{\text{nnc}} \left(\frac{C}{\mathbf{r}_{ij}} \right)^{12} \quad (11)$$

For potential functions, $V_z^{(\alpha)}$, $V_{\text{nc}}^{(\alpha)}$ and V_{ij}^{nnc} , we employ the same functions as those used by Clementi *et al.*[18]. The superscript α is 1 or 2 that represents reference structures. Parameters with superscript 1(2) are constants, of which values are taken from the corresponding variables in structure-1 or in structure-2. For local interaction terms (bond-length, bond-angle, dihedral-angle), the potential energy for each set of beads takes smaller of $V^{(1)}$ and $V^{(2)}$. For example, length of i -th bond is $b_i^{(1)}$ in structure-1 and is $b_i^{(2)}$ in structure-2, then the potential energy for this bond is $k_b \min\{(b_i - b_i^{(1)})^2, (b_i - b_i^{(2)})^2\}$. We define that i -th and j -th amino acids are in the “native contact pair” of structure-1(2) if one of the non-hydrogen atoms in the j -th amino acid is within 6.5 Å distance from one of non-hydrogen atoms in the i -th amino acid at the structure-1(2). The interaction potential for each native-contact pair $i-j$, takes smaller of $V_{\text{nc}}^{(1)}(\mathbf{r}_{ij})$

and $C_{12}V_{\text{nc}}^{(2)}(\mathbf{r}_{ij})$. If a residue pair $i-j$ is native-contact-pair in structure-1(2) but is not in structure-2(1), the interaction potential between i and j -th residue is Lenard-Jones potential, $V_{\text{nc}}^{(1(\text{or}2))}(\mathbf{r}_{ij})$, that has single minimum. C_{12} is the ratio of potential depth of structure-2 to that of structure-1 (Fig.7). Here, since we are to perform structural change simulation from structure-2 to structure-1, that is, we take structure-1 as the final stable structure, we assign a value smaller than 1 to C_{12} . In the present work, we take $C_{12} = 0.8$ and other parameters is the following; $k_b = 100.0$, $k_\theta = 20.0$, $k_\phi = 1.0$, $k_{\text{nc}} = k_{\text{nnc}} = 0.25$ and $C = 4.0$. The cut-off length for calculating $V_{\text{nc}}^{(z)}$ is taken as $2r_{ij}^{(z)}$.

We use the model for discussing structural relaxation of the myosin motor domain from the pre-powerstroke state to the near-rigor state. So structure-1 and 2 correspond to near-rigor and pre-powerstroke structure, respectively. For the purpose of understanding mechanism of acto-myosin motor, it is desirable to study conformational change to the rigor state. However, currently no x-ray crystal structure is available for true rigor complex with actin. So we use near-rigor state instead, 1Q5G[20] which is nucleotide free structure of *Dictyostelium discoideum* myosin II. Although a few nucleotide free structures of myosin II have been solved, only 1Q5G is regarded as the near-rigor state, because both switch I and switch II are in the open position. We choose 1VOM[21] as pre-powerstroke structure, which includes ADP-P_i analog (ADP·VO₄) in the nucleotide binding site. While 1Q5G consists of residues 2-765 without gap region, 1VOM includes only residues 2-747 and it has gap regions where structure is undetermined by x-ray crystallography. So we use structures of residues 2-747 for simulations. Potential functions for local-interactions in the gap region are assigned minima corresponding to the near-rigor conformation.

Nucleotide molecule (ADP·VO₄ in 1VOM) is also included in the simulation as a coarse-grained chain (Fig. 2) as well as coarse-grained protein. The coarse-grained ADP·VO₄ is represented as a short linear chain constituted of 5 beads, corresponding to purine base, sugar(ribose), 2 phosphates and VO₄(phosphate analog). The intra-nucleotide interaction is defined as

$$U_n = \sum_k k_b (\|\mathbf{r}_{k+1} - \mathbf{r}_k\| - \| \mathbf{r}_{k+1}^{(2)} - \mathbf{r}_k^{(2)} \|)^2 + \sum_k k_b (\|\mathbf{r}_{k+2} - \mathbf{r}_k\| - \| \mathbf{r}_{k+2}^{(2)} - \mathbf{r}_k^{(2)} \|)^2. \quad (12)$$

The interaction potential between protein and nucleotide is similar to that between nonlocal residues in the protein. Here, we consider the case that only structure-2 includes nucleotide; so the potential function has only a single well (standard Lenard-Jones potential). We define that i -th residue of the protein and k -th bead in the nucleotide chain is in “native-contact” in pre-powerstroke conformation when one of the non-hydrogen atoms in the k -th bead (base or sugar of Pi) is within 4.5 Å distance from one of non-hydrogen atoms in the i -th amino acid. We call residues which form native-contacts with

nucleotide as “nucleotide-contact residues”.

$$U_{\text{p-n}}(\mathbf{r}_{ik}) = \sum_{i,k}^{\text{native contact}} \left\{ k_{\text{p-n}} \left[5 \left(\frac{r_{ik}^{(2)}}{\mathbf{r}_{ik}} \right)^{12} - 6 \left(\frac{r_{ik}^{(2)}}{\mathbf{r}_{ik}} \right)^{10} \right] \right\}. \quad (13)$$

where i stands for i -th residue and k stands for k -th bead in the nucleotide chain.

Dynamics of the protein is simulated using the Langevin equation at a constant temperature T ,

$$m_i \dot{\mathbf{v}}_i = \mathbf{F}_i - \gamma \mathbf{v}_i + \xi_i \quad (14)$$

where \mathbf{v} is the velocity of the i -th bead, and a dot represents the derivative with respect to time t and thus $\mathbf{v}_i = \dot{\mathbf{r}}_i$. \mathbf{F}_i and ξ_i are systematic and random forces acting on the i -th bead, respectively. The systematic force \mathbf{F}_i is derived from the effective potential energy U , $\mathbf{F}_i = -\partial V/\partial \mathbf{r}_i$. ξ_i is a Gaussian white random force, which satisfy $\langle \xi_i \rangle = 0$ and $\langle \xi_i(t) \xi_j(t') \rangle = 2\gamma T \delta_{ij} \delta(t-t') \mathbf{1}$, where the bracket denotes the ensemble average and $\mathbf{1}$ is a 3×3 unit matrix. For numerical integration of the Langevin equation, we use an algorithm by Honeycutt and Thirumalai [26]. We use $\gamma = 0.25$, $m_i = 1.0$, and the finite time step $\Delta t = 0.02$.

For a given protein conformation Γ , we regard that the “native contact of structure-1(2)” between i and j is formed if the C_α distance $r_{ij} = \|\mathbf{r}_{ij}\|$ satisfies $0.8r_{ij}^{(1)} < r_{ij} < 1.2r_{ij}^{(1)}$ ($0.8r_{ij}^{(2)} < r_{ij} < 1.2r_{ij}^{(2)}$).

Simulations are started from the pre-powerstroke structure. Initial positions of residues in the gap regions of 1VOM were set randomly under the condition that the bond-length is 3.8 Å. Initial velocities of each beads were given to satisfy the Maxwell distribution. Temperature is set lower than the folding temperature to structure-1

We also make “the nucleotide-free and constrained simulation”, in which the nucleotide is not explicitly included but the relative positions of the “nucleotide-contact residues” are constrained by virtual bonds in a all-to-all manner to keep the pre-powerstroke form instead. The natural length of virtual bonds $i-j$, $r_{ij}^{(2)}$ is the C_α distance between i and j -th residues in pre-powerstroke conformation (structure-2). Total effective potential energy was $U_p + U_{\text{constraint}}$, and

$$U_{\text{constraint}} = \sum_{j < i}^{\text{nucl.-contact pair}} k_{\text{constraint}} (r_{ij} - r_{ij}^{(2)})^2, \quad (15)$$

where $k_{\text{constraint}} = 1.0$.

Acknowledgments

We thank Shoji Takada and Toshio Yanagida for many helpful suggestions. This work was supported by Core Research for Evolutional Science and Technology of Japan Science and Technology Agency.

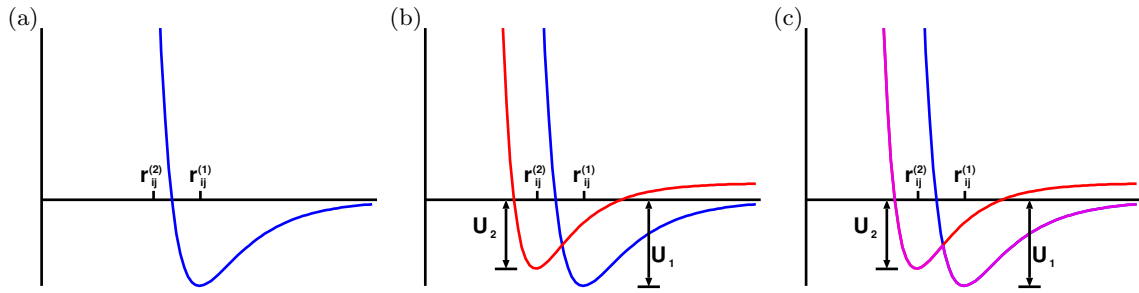


FIG. 7: Go-potential: magenta line is dual Go-potential energy profile for the $i-j$ pair. $C_{12} = U_2/U_1$.

[1] M. A. Geeves and K. C. Holmes, *Annual Review of Biochemistry* **68**, 687 (1999).

[2] K. Kitamura, M. Tokunaga, S. Esaki, A. H. Iwane, and T. Yanagida, *BIOPHYSICS* **1**, 1 (2005).

[3] J. A. Spudich, *Nat. Rev. Mol. Cell Biol.* **2**, 387 (2001).

[4] T. Yanagida, T. Arata, and F. Oosawa, *Nature* **316**, 366 (1985).

[5] R. D. Vale and F. Oosawa, *Advances in biophysics* **26**, 97 (1990).

[6] F. Julicher, A. Ajdari, and J. Prost, *Reviews of Modern Physics* **69**, 1269 (1997), URL <http://link.aps.org/abstract/RMP/v69/p1269>.

[7] P. Reimann, *Physics Reports* **361**, 57 (2002).

[8] C. Veigel, J. E. Molloy, S. Schmitz, and J. Kendrick-Jones, *Nat. Cell. Biol.* **5**, 980 (2003).

[9] C. Veigel, S. Schmitz, F. Wang, and J. R. Sellers, *Nat. Cell. Biol.* **7**, 861 (2005).

[10] D. Altman, H. L. Sweeney, and J. A. Spudich, *Cell* **116**, 737 (2004).

[11] A. F. HUXLEY, *Progress in biophysics and biophysical chemistry* **7**, 255 (1957).

[12] Q. Cui, G. Li, J. Ma, and M. Karplus, *Journal of Molecular Biology* **340**, 345 (2004).

[13] M. Ikeguchi, J. Ueno, M. Sato, and A. Kidera, *Phys. Rev. Lett.* **94**, 078102 (2005).

[14] W. Zheng and S. Doniach, *PNAS* **100**, 13253 (2003).

[15] N. Koga and S. Takada, *PNAS* **103**, 5367 (2006).

[16] N. Go, *Annu. Rev. Biophys. Bioeng.* **12**, 183 (1983).

[17] J. N. Onuchic, Z. Luthey-Schulten, and P. G. Wolynes, *Annual Review of Physical Chemistry* **48**, 545 (1997).

[18] C. Clementi, H. Nymeyer, and J. N. Onuchic, *Journal of Molecular Biology* **298**, 937 (2000).

[19] N. Koga and S. Takada, *Journal of Molecular Biology* **313**, 171 (2001).

[20] T. F. Reubold, S. Eschenburg, A. Becker, F. J. Kull, and D. J. Manstein, *Nat. Struct. Biol.* **10**, 826 (2003).

[21] C. A. Smith and I. Rayment, *Biochemistry* **35**, 5404 (1996).

[22] A. Ishijima, H. Kojima, T. Funatsu, M. Tokunaga, H. Higuchi, H. Tanaka, and T. Yanagida, *Cell* **92**, 161 (1998).

[23] E. M. D. L. Cruz and E. M. Ostap, *Current Opinion in Cell Biology* **16**, 61 (2004).

[24] J. R. Sellers, *Biochem. Biophys. Acta* **1496**, 3 (2000).

[25] W. M. Shih, Z. Gryczynski, J. R. Lakowicz, and J. A. Spudich, *Cell* **102**, 683 (2000).

[26] J. D. Honeycutt and D. Thirumalai, *Biopolymers* **32**, 695 (1992).